

Damaging and Cracks in Thin Mud Layers.

Raffaele Cafiero¹, Guido Caldarelli², Andrea Gabrielli³

¹ PMMH Ecole Sup. de Physique et de Chimie Industrielles (ESPCI), 10, rue Vauquelin-75231 Paris Cedex 05 France

² INFN Sezione di Roma1, Dipartimento di Fisica, Università di Roma “La Sapienza”, P.le A. Moro 2, I-00185 Roma, Italy

³ Laboratoire de Physique de la Matière Condensée, Ecole Polytechnique, 91128-Palaiseau Cedex, France

(March 14, 2021)

We present a detailed study of a two-dimensional minimal lattice model for the description of mud cracking in the limit of extremely thin layers. In this model each bond of the lattice is assigned to a (quenched) breaking threshold. Fractures proceed through the selection of the part of the material with the smallest breaking threshold. A local damaging rule is also implemented, by using two different types of weakening of the neighboring sites, corresponding to different physical situations. Some analytical results are derived through a probabilistic approach known as Run Time Statistics. In particular, we find that the total time to break down the sample grows with the dimension L of the lattice as L^2 even though the percolating cluster has a non trivial fractal dimension. Furthermore, a formula for the mean weakening in time of the whole sample is obtained.

05.20-y, 62.20.Mk

I. INTRODUCTION

In this paper we present a careful and detailed study of a minimal fracture model that has been introduced at the aim of describing the main features of paint dessication-like phenomena [1]. The purpose of this work is to focus on the statistical properties of these phenomena on the basis of a recent experimental work [2]. Following the results of this work, we assumed that the main source of stress is given by the *local* friction between the layer of material and the bottom surface of the container. Moreover, it has been noticed that the characteristic size of crack patterns varies linearly with the layer thickness. In the limit of zero thickness *crack patterns lose their polygonal structure* (the characteristic size of the polygons is zero) and become *branched fractals*.

In order to model this behavior, a minimal automaton lattice model, inspired by Invasion Percolation [3] and by the vectorial and scalar models described in [4,5], has been recently introduced by the authors [1]. Here, we present an extended report of the study described in [1], with a detailed description of the analytical calculations a new numerical and theoretical results. All the models for *quasi-static* fractures, describe crack evolution through a non-local Laplacian field (electric field, electric current) acting on a solid network of bonds or sites [5]. In others the stress field evolves by keeping minimum the energy of the system. In such a case the components of the obtained vectorial equations are similar to the equations describing the action of a Laplacian field [4]. In this model, instead, no explicit field is present. The effect of the stress is represented by an extremal breaking rule and *local* random breaking thresholds: at each time step, the bond with the smallest threshold is removed from the lattice. Short ranged correlations are introduced through a damaging of the non-broken nearest neighbors bonds of the just removed bond. According to the kind of fracture we deal with, one can introduce different types of

damaging. In this paper two limiting cases are studied. This model is inspired by the above cited experimental observations [2] that, in an extremely thin layer of mud or paint, the only source of stress is the *local* friction with the container. Moreover, since the drying mud is a mixture of a liquid and a solid (usually amorphous) phase, no long range stress relaxation is present, although the growing crack can affect the properties of the medium in its neighborhood. Some important physical properties of the model are explained by using an approach based on the Run Time Statistics (RTS) scheme [6]. In particular, we are able to compute some relevant quantities, such as the evolution of the breaking probability, and of the probability distribution of breaking thresholds.

The paper is so organized. In Sec. II the model is described. In Sect. III the results of numerical simulations are presented. In Sect. IV the model is studied analytically and theoretical and numerical results are compared.

II. THE MODEL

A square lattice is considered and a quenched random variable x_i is assigned to each bond i . The x_i 's are independently extracted from a uniform probability density between 0 and 1. At each time-step t , the unbroken bond in the lattice with the lowest value of the variable is broken (removed). Then damage (weakening) is applied, in a way explained below, to the unbroken nearest neighbors (n.n.) of the just removed bond. After having introduced the damaging, the breaking and damaging steps are repeated until a connected, percolating, subset (infinite cluster) of removed bonds appears, dividing the system into two disconnected parts.

Before explaining the definition of damaging, it is necessary to introduce some notations. The set of broken bonds up to time t is indicated with C_t , and the set of non-broken bonds with ∂C_t . The number of bonds be-

longing to C_t is $\|C_t\| = t$, while $\|\partial C_t\| = N - t$ (where N is the total number of bonds in the lattice), in fact ∂C_t is composed by the whole lattice minus the bonds in C_t . The definition of C_t is independent of the model. That of ∂C_t , instead, can differ a lot from a model to another; for instance in Invasion Percolation (IP) it is simply given by the set of nearest neighbors of the bonds in C_t .

Two different kinds of weakening of the unbroken neighbors are studied: Either by direct weakening or by re-distribution of the “stress”. In the first case (rule **1**), the unbroken n.n. are weakened, by extracting a new threshold x'_i between 0 and the former value x_i . In this case an average weakening of one half of the former value at time is obtained. In the second case (rule **2**), instead, each neighbor has a threshold weakened by a fraction of the threshold of the bond just removed. Both cases mimic the damaging produced by the enhancement of the stress nearby crack tips: the first case refers to a situation where stochasticity (thermal fluctuations) is important in the determination of the new thresholds [7], the second case refers to a deterministic effect around the crack tip. From the point of view of mud cracking, the two-dimensional lattice represents a very thin layer of mud (or paint), and quenched disorder *accounts for local stress induced by inhomogeneous desiccation of the sample*. Since the evolution of cracks in mud desiccation is assumed to be a slow process, the dynamics is assumed to be *quasi-static*, i.e. one microscopical breaking with relative damaging for each time-step. Some authors correctly point out that otherwise time-dependent effects and a non-equilibrium dynamics are relevant in crack propagation [8].

In this model the explicit presence of an external field (applied stress) and of the response of the material (strain of bonds) have been eliminated. The only quantity present is the breaking threshold, the dynamics of which is chosen to reproduce the evolution of cracks. This simulates the presence of a local stress field, acting not on the boundaries but directly on each bond. Our assumption is based on the experimental results in Ref. [2], where, as the mud layer becomes thinner, only the inhomogeneities drive the nucleation of cracks. Furthermore, the hypothesis of crack developing under the same state of strain not only is usually applied in the presence of thermal gradients [9], but is also commonly reported in experiments of loading of softened material [10–12]. Hence, such a model is particularly suitable to describe, for example, paint drying, where the stress applied to the painted surface depends on the local action of external conditions (density gradient in the paint). Moreover, its simplicity allows us to study analytically its properties, which is a non common feature for fracture models.

III. NUMERICAL RESULTS

Numerical simulations, with cylindrical symmetry (periodic boundary conditions in the horizontal direction) for various system sizes L have been performed. The dynamics stops as soon as a crack spanning the system in the vertical direction appears. Both damaging rules are implemented, and they are discussed in parallel. Despite the simplicity of the dynamical rules, the results are rather interesting. We have computed the fractal dimension of the percolating cluster, the distribution of the size of clusters of broken bonds, the avalanche size-distribution (in order to check if long range temporal correlations are present), and the probability distribution of the breaking thresholds at the percolation time. An avalanche can be defined as an ensemble of causally and geometrically connected breakdowns (see below for a rigorous definition). Under this respect the size-distribution of such avalanches represents the probability of a large or small response of the system to an external solicitation. For example a power law distribution represents a critical state of the system where the response has not a characteristic size.

The fractal dimension D_f of the percolating cluster is computed using the box-counting method. The analysis is restricted to the spanning cluster to reduce the finite size effects present for the smaller clusters. The results of the box-counting analysis are reported in Table I for the different sizes and for the two damaging rules. The values of D_f for the two damaging rules coincide within the error bars.

The connected clusters of broken bonds are identified with a standard cluster counting procedure, based on the Hoshen-Kopelman algorithm [13]. Also the distribution of finite clusters is nontrivial, showing a clear power law with exponent $\tau_c = 1.54(2)$ (see Fig. 1(a)) for rule **1** and $\tau_c = 1.57(3)$ for rule **2**. The plots labelled with (b) in Fig. 1 refer to the avalanche size distribution. This quantity is interesting with respect to recent experiments [14] and models [4,5] where a power law behavior of the acoustic emission has been related to Self-Organized Criticality (SOC) [15]. The presence of a SOC-like behavior would mean that the dynamics of fractures itself leads the sample to a steady state where small variation of the external field can trigger reaction at any length-scale. In particular the external field in this case is the applied stress, and the response of the sample can be considered as the energy released (acoustic emission) by one avalanche of cracks, where avalanche means a causally and geometrically connected series of breakdowns. In this oversimplified model the external stress can be considered constant, since the only change after any single breakdown is due the damaging of the n.n.. Consequently, in this work the size of an avalanche is monitored as a measure for the acoustic emission. An avalanche can be defined as fol-

lows. Let us suppose that a bond i grows (i.e. it is broken) at time t ; this is the *initiator* of an avalanche, which is defined as the set of events geometrically and causally connected to the initial one (bond i). “Causal” connection refers to the weakening following any bond breaking. In particular, when bond i grows at time t , the avalanche goes on at time $t + 1$ if a unbroken first neighbor bond j of i is removed. At time $t + 2$ the avalanche goes on if a bond k grows where k is a unbroken first neighbor of i or j and so on. A linear-log plot of the probability distribution of avalanche size, versus sample size L is shown in Fig. 1b. After a power law transient, an exponential distribution is reached, indicating that a characteristic size exists for the avalanches. One can note that both for weakening rule **1** and weakening rule **2** simulations give qualitatively similar results, although for rule **2** the characteristic time of avalanches is smaller. This is easily explained, since the damaging rule **2** is less strong than rule **1**, and, consequently, the causal connection between subsequent breaking events is weaker.

This result for avalanches is similar to those obtained for a scalar model of Dielectric Breakdown, but differs from the avalanche behavior in models of fracture [4,5]. The explanation of this behavior is motivated by two arguments. Firstly, in the present definition of an avalanche the threshold is changed only for the n.n.. This introduces a typical length scale, while other definitions consider as the threshold the ratio between local field and resistivity, thus giving the possibility of large scale correlations. Secondly, in this model broken bonds *are removed from the system*. This represents a substantial difference with many SOC models with quenched disorder presented in the literature. For example, in a simple toy model of SOC due to Bak and Sneppen [16] (where a similar refresh of thresholds is present) the dynamics produces clear power laws in the avalanche distribution. There, each site (species) deleted is replaced by a new one and is not definitively removed. In our model, instead, the number of candidates ∂C_t to be broken at each time-step decreases in time. This is a crucial point, since indeed power law behavior in the presence of a scalar field seems to be related to a “reconstructing rule” that allows one to deal with a system where removed bonds are replaced by new ones. Therefore, only in the case of plastic deformation, one is in the presence of a steady state, as correctly pointed out by Ref. [5].

Therefore, the fractal dimension, the cluster size distribution and, to some extent, the avalanche size distribution seem to be universal with respect to the two different local damaging rules. In the next section the study will focus on some quantities which, instead, are not universal and reproduce the evolution of the mechanical properties of the material during the fracturing dynamics. These quantities are the average probability density of breaking thresholds, or histogram, $\phi_t(x)$, and as a by-product the mean breaking threshold $\langle x \rangle(t)$, which expresses the

average resistance to breaking, or rigidity, of the system at time t . These quantities will be studied both numerically, and analytically, by using a probabilistic tool called Run Time Statistics (RTS) [6].

IV. RTS DERIVATION OF THE AVERAGE WEAKENING OF THE MATERIAL

As seen above, the evolution of the crack is described by a quasi-static extremal dynamics in a medium with quenched disorder. The most important question for a theoretical comprehension of the model is: which is the source of the spatio-temporal correlations developed by the dynamics? As pointed in [6] in relation to Invasion Percolation (IP), the source can be found in the memory effects developed by the evolution of the dynamics itself via an interplay between dynamical rules and quenched disorder.

This can be simply realized observing that the knowledge of the growth history up to a time t , provides information about the probability distribution and the correlations of the random bond-thresholds. This information has to be added to the original information that the thresholds are independently extracted from the uniform probability density in the interval $[0, 1]$. Moreover this information influences the probabilities of the different possible continuations of the dynamics for larger time. This memory effects can be studied using carefully the notion of conditional probability. This kind of approach to growth dynamics with quenched disorder has been developed in [6,17], with particular reference to IP. This peculiar probabilistic algorithm is called *Run Time Statistics* (RTS). A particular modification of this tool is presented here taking into account the damaging mechanism, which is not present in IP-like models. Finally, RTS is used in order to predict analytically some relevant quantities as the evolution of both the average probability density of breaking thresholds of unbroken bonds and of the mean resistance to breakdown $x(t)$ of the material.

Here we provide directly the final RTS formulas together with a brief sketch about their meaning. A detailed derivation of the analytical results of this section is given in Appendix A. The RTS approach permits mainly to answer the following two questions, once given a certain time-ordered geometrical path followed by the dynamics up to time t :

1. which is the *effective* probability density function of the variables x_i of the lattice conditioned to the knowledge of this fixed past dynamical history;
2. which is the conditional probability of any further growth event at the next time-step.

In order to introduce operative formulas, let us think to know the “one-bond” effective probability density functions $p_{i,t}(x)$ (conditioned to the past dynamical history)

for each non-broken bond i . As it is clarified in Appendix A, this “one-bond” formulation of RTS is an approximate of the rigorous one. However, as shown in [18], it is a good approximation when the number of random numbers is large (as in this case).

First of all one can write [6] the breaking probability $\mu_{i,t}$ for each bond i at that time-step:

$$\mu_{i,t} = \int_0^1 dx p_{i,t}(x) \left[\prod_{k(\neq i)}^{\partial C_t} \int_x^1 dy p_{k,t}(y) \right], \quad (1)$$

where ∂C_t is the whole set of unbroken bonds. Note that at time t the number of bonds in ∂C_t is $(2L^2 - t)$, i.e., the total number $2L^2$ of bonds in a square lattice of side L minus the number of broken bonds before time t . Eq. (1) expresses nothing else than the effective probability that x_i is the minimum in the set ∂C_t conditioned to the past history. The next important step is to update each $p_{j,t}(x)$ by conditioning them to this latest growth event. In this way one obtains the $p_{j,t+1}(x)$ ’s conditioned to the history up to the time-step $t+1$. The effective probability density at time $t+1$ of the latest grown bond i is usually called $m_{i,t+1}(x)$, in order to distinguish it from the densities of still unbroken bonds. It is given by

$$m_{i,t+1}(x) = \frac{1}{\mu_{i,t}} p_{i,t}(x) \left[\prod_{k(\neq i)}^{\partial C_t} \int_x^1 dy p_{k,t}(y) \right]. \quad (2)$$

Eq. (2) (multiplied by dx) gives the “effective” probability that $x \leq x_i \leq x + dx$, conditioned to the past fixed dynamical history (time-ordered path) up to time $t+1$: the “memory” of the history up to time t is “recorded” in the set of functions $p_{k,t}(x)$, where k runs over all the bond belonging to ∂C_t , while the last step is recorded in the particular functional relationship between $m_{i,t+1}(x)$ and the set $\{p_{k,t}(x)\}$ itself. This relationship is imposed by the order relation among the interface variable x_k , i.e. by the fact that x_i is the minimum in ∂C_t . Note that, once a bond is broken, it does not participate anymore to the dynamics. For this reason, the “effective” probability density function of its threshold does not change anymore in time and is given definitely by Eq. (2).

For the remaining bonds one has to distinguish among the unbroken bonds far away from the bond i and the unbroken nearest neighbors bonds, which will be weakened by the growth of bond i . The updating rules, for the two different mechanisms of damaging, differ only for this last set of bonds. For the non-weakened bonds, one has in both cases the following updating equation:

$$p_{j,t+1}(x) = \frac{1}{\mu_{i,t}} p_{j,t}(x) \int_0^x dy p_{i,t}(y) \left[\prod_{k(\neq i,j)}^{\partial C_t} \int_y^1 dz p_{k,t}(z) \right] \quad (3)$$

The updating equations for the weakened bonds are instead the following:

(1) For the damaging mechanism **1**:

$$p_{j,t+1}(x) = \frac{1}{\mu_{i,t}} \int_0^1 dy \frac{1}{y} \theta(y - x) p_{j,t}(y) \times \int_0^y dz p_{i,t}(z) \left[\prod_{k(\neq i,j)}^{\partial C_t} \int_z^1 du p_{k,t}(u) \right]. \quad (4)$$

(2) For the damaging mechanism **2** (see Appendix A):

$$p_{j,t+1}(x) = \frac{1}{\mu_{i,t}} \int_0^1 dy \left[\prod_{k(\neq i,j)}^{\partial C_t} \int_y^1 dz p_{k,t}(z) \right] p_{i,t}(y) p_{j,t}\left(x + \frac{y}{n_{i,t}}\right) \times \theta\left(\frac{n_{i,t}}{n_{i,t} - 1} x - y\right) \theta(n_{i,t}(1 - x) - y) \quad (5)$$

Note that the main difference between Eq. (4) and Eq. (5) is due to the fact that the number of n.n. $n_{i,t}$ of the bond i at time t appears explicitly only in the latter, i.e. only in the second model (rule **2**) the damaging is an explicit function of the geometry, while in the former (rule **1**) the damaging is a “one-bond” process.

Eqs. (1-3) coincide with the ones introduced for the RTS approach to IP (apart from the different definition of the growth interface ∂C_t). Eqs. (4), (5), instead, are new and account for the n.n. weakening. Eqs. (1-5) allow one to study the extremal deterministic dynamics as a kind of stochastic process with memory. In particular, $\mu_{i,t}$ can be used to evaluate systematically the statistical weight of a fixed time-ordered growth path, while the $p_{j,t}(x)$ ’s store information about the growth history.

A very important quantity to characterize the properties of the dynamics is the empirical distribution (or histogram) of unbroken thresholds. This quantity is defined as:

$$h_t(x) = \sum_{j \in \partial C_t} p_{j,t}(x) \quad (6)$$

where, $h_t(x)dx$ is the number of non-broken bonds between x and $x + dx$ at time t , conditioned to the past dynamical history.

Considering the effect of the growth of bond i at time t on this quantity, one gets

$$h_{t+1}(x) = h_t(x) - m_{i,t+1}(x) - \sum_{j(i)} p_{j,t}(x) + \sum_{j(i)} p_{j,t+1}(x) \quad (7)$$

where $j(i)$ indicates the sum over the $n_{i,t}$ unbroken n.n. of i . Moreover, $m_{i,t+1}(x)$ and $p_{j,t+1}(x)$ are given respectively by Eq. (2) and Eqs. (3), (4) (5) for rule **2**. Being the histogram an almost self-averaging quantity of the model in the large time limit, one can evaluate its

shape in the “typical” realization of the dynamics taking the average over all the possible histories up to time $t + 1$. The notation $\langle \dots \rangle$ is introduced to indicate for this average. The l.h.s. of Eq. (7) can be computed as

$$\langle h_{t+1}(x) \rangle = \|\partial C_{t+1}\| \phi_{t+1}(x) = [N - (t+1)] \phi_{t+1}(x), \quad (8)$$

where $N = 2L^2$ is the total number of bonds in the lattice and $\phi_t(x)$ represents the average thresholds density function over the unbroken bonds at time t (normalized to 1), i.e. $\phi_t(x) = p_{k,t}(x)$ where k is a generic interface bond. For the r.h.s. of Eq. (7) the main difficulty arises in the evaluation of $\langle m_{i,t+1} \rangle$ and $\langle \sum_{j(i)} p_{j,t+1}(x) \rangle$. Following [6], one can write

$$\langle m_{i,t+1} \rangle \simeq (N - t) \phi_t(x) \left[1 - \int_0^x dy \phi_t(y) \right]^{N-t-1} \quad (9)$$

In obtaining Eq. (9), we used the definition of $\phi_t(x)$ and the following approximation:

$$\left\langle \prod_{k \in \partial C_t} p_{k,t}(x_k) \right\rangle = \prod_{k \in \partial C_t} \langle p_{k,t}(x_k) \rangle = \prod_{k \in \partial C_t} \phi_t(x_k). \quad (10)$$

Using again the definition of $\phi_t(x)$, one gets

$$\left\langle \sum_{j(i)} p_{j,t}(x) \right\rangle = n_t \phi_t(x), \quad (11)$$

where $n_t = \langle n_{i,t} \rangle$. Using Eq. (4), corresponding to the weakening rule **1**, and the approximations given by Eq. (10), one has

$$\begin{aligned} \left\langle \sum_{j(i)} p_{j,t+1}(x) \right\rangle &= \frac{n_t(N-t)}{N-t-1} \int_x^1 dy \frac{\phi_t(y)}{y} \times \\ &\times \left\{ 1 - \left[1 - \int_0^y dz \phi_t(z) \right]^{N-t-1} \right\}. \end{aligned} \quad (12)$$

The equation for the $\phi_{t+1}(x)$ for rule **1** will finally read:

$$\begin{aligned} \phi_{t+1}(x) &= \frac{N-t-n_t}{N-t-1} \phi_t(x) + \\ &- \frac{N-t}{N-t-1} \phi_t(x) \left[1 - \int_0^x dy \phi_t(y) \right]^{N-t-1} + \\ &+ n_t \frac{N-t}{(N-t-1)^2} \int_x^1 dy \frac{\phi_t(y)}{y} \times \\ &\times \left\{ 1 - \left[1 - \int_0^y dz \phi_t(z) \right]^{N-t-1} \right\} \end{aligned} \quad (13)$$

Note that even at percolation time $N - t$ is a large number. For this reason terms in Eq. (13) containing the term $\left[1 - \int_0^x dy \phi_t(y) \right]^{N-t-1}$ are negligible for x such

that $\int_0^x dy \phi_t(y)$ is finite (i.e. larger than $1/(N - t)$). It is easy to show that the continuum limit of Eq. (13), for such values of x , is invariant under the rescaling $L \rightarrow aL$ (i.e. $N \rightarrow a^2 N$) and $t \rightarrow a^2 t$. This result is based on the assumption that:

$$n_t(L) = n_{a^2 t}(aL) \quad (14)$$

The numerical simulations suggest the following scaling form for $n_t(L)$ (see Fig. 2):

$$n_t(L) = n_{max} \left[\frac{1}{1 + t/AL^2} \right]^\beta, \quad (15)$$

where $\beta = 0.23(2)$, $A = 0.030(2)$ and $n_{max} = 6$ is the lattice coordination number. This form for n_t satisfies Eq. (14).

The study of the weakening rule **2** is quite similar. Eqs. (1-3) keep the same, while the conditioned probability density for the weakened bonds is given by Eq. (5).

By following the same steps as above, the following equation for the $\phi_{t+1}(x)$ is obtained:

$$\begin{aligned} \phi_{t+1}(x) &= \frac{N-t-n_t}{N-t-1} \phi_t(x) + \\ &- \frac{N-t}{N-t-1} \phi_t(x) \left[1 - \int_0^x dy \phi_t(y) \right]^{N-t-1} + \\ &+ n_t \frac{N-t}{N-t-1} \int_0^1 dy \left[1 - \int_0^y dz \phi_t(z) \right]^{N-t-2} \phi_t(y) \times \\ &\times \phi_t \left(x + \frac{y}{n_t} \right) \theta \left(\frac{n_t}{n_t-1} x - y \right) \theta(n_t(1-x) - y) \end{aligned} \quad (16)$$

All the assumptions we made for the case **1**, including the scaling *ansatz* given in Eq. (14), are valid for case **2**. In particular, from numerical simulations, one can find the following behavior for $n_t(L)$ (see Fig. 3) :

$$n_t(L) \simeq n_{max} \exp \left(-\frac{t}{AL^2} \right). \quad (17)$$

The analytical study of both kinds of weakening allows to make three important predictions: **(1)** Firstly, we find both theoretically, from the numerical solution of Eqs.(13, 16), and from the numerical simulations of the model, a discontinuity in the histogram (see Fig. 4 and 5), indicating that the system evolves in such a way as to remove all bonds with threshold smaller than some critical value x_c . **(2)** Second, from the symmetry properties of Eqs. (13, 16), we deduce that the number $t_{sp}(L)$ of broken bonds at the percolation time is proportional to L^2 , even though the percolating cluster is fractal. This result, confirmed by numerical simulations (see Fig. 6a, Fig. 7a), and compatible with the scaling function (15) for $n_t(L)$, is deduced supposing that at the percolation time the shape of the histogram is independent of L , an assumption which fits well with the numerical histogram

(see Fig. 4a and Fig. 5a). **(3)** Finally, we present an approximated result for the dynamical behavior of the average value (over the unbroken bonds) of the thresholds $\langle x \rangle(t)$. This quantity can be seen as a characterization of the average resistance of the material in time.

In order to find the evolution equation of $\langle x \rangle(t)$ for the damaging rule **1**, it is enough to multiply both sides of, respectively, Eq. (13) and Eq. (16) for x and integrate them in the whole interval $[0, 1]$. Then one finds:

$$\langle x \rangle(t+1) = \left(1 - \frac{n_t - 2}{2(N - t - 1)}\right) \langle x \rangle(t) + \frac{1 + n_t/[2(N - t - 1)]}{N - t - 1} \int_0^1 dx \left[1 - \int_0^x dy \phi_t(y)\right]^{N-t}. \quad (18)$$

For the damaging rule **2**, the way to find the equation for $\langle x \rangle$ is even simpler. In fact, it is enough to consider that at each time step, the global effect on $\langle x \rangle$ is equivalent to remove two bonds with the resistance equal to the minimal one at that time. Therefore, one can write:

$$\langle x \rangle(t+1) = \left(1 + \frac{1}{N - t - 1}\right) \langle x \rangle(t) + \frac{2}{N - t - 1} \int_0^1 dx \left[1 - \int_0^x dy \phi_t(y)\right]^{N-t}. \quad (19)$$

For rule **1**, it is simple to see, from Eq. (18), that $\langle x \rangle(t+1) < \langle x \rangle(t)$ until $n_t > 2$ (which is verified for all the times). This means that on average the medium weakens during the evolution even if the weakest bond is removed at any time step. This is due to the fact that, in this case the weakening of the neighbors of the weakest interface bond has a stronger effect on the material than the removal of the weakest bond itself. For the rule **2**, instead, one finds that $\langle x \rangle(t+1) > \langle x \rangle(t)$, if $\langle x \rangle(t)$ is larger than the double of the average minimal threshold, and, due to the extremal nature of the dynamics, this is verified always in the large N limit, i.e. in the limit of a large number of bonds in the interface at any time-step. This means that in this second case, damaging is not strong enough to allow a global weakening of the system, which becomes more and more rigid. This is reasonable since in rule **2** the stress on the weakest bond is redistributed to the nearest neighbors, and the total initial stress is conserved, while in rule **1** there is not total stress conservation. In other words, in the model with rule **1** the damaging is a multiplicative effect, i.e. the damaging is proportional to the old threshold (which can be big), in the model with rule **2** the damaging is quite reduced by the fact that at each time-step it is proportional to the minimal threshold in the whole system. In Figs. 6b, 7b the time evolution of $\langle x \rangle(t)$ obtained from computer simulations is compared with the theoretical prediction. Our analytical results are in good agreement with numerical simulations. For rule **2**, numerical simulations of the histogram evidenciate a low x tail below the critical

threshold, which tends to disappear as the system size grows, and a non zero slope of the part just above the critical threshold. The first one is a clear finite size effect, which is less important in the simulations of rule **1**, because for rule **1** the critical threshold is very small. Of course, such a finite size effect is absent in the theoretical results, as in all mean field (MF) approaches. The second effect could be due to spatial correlation induced by the damaging rule **2**, which in the analytical approach are neglected. This second effect does not disappear as the system size grows. Consequently the agreement between the numerical simulations of $\langle x \rangle(t)$ and Eq. (19) is less good than for rule **1**. The numerical $\langle x \rangle(t)$, mainly because of the nonzero negative slope of $\phi(x)$ above x_c , is a bit smaller than the theoretical prediction.

With respect to real fracturing processes the behavior of the average resistance $\langle x \rangle(t)$ obtained with rule **2** is more realistic, since in real materials one usually observes that the material during micro-cracks formation becomes more rigid, although more fragile, since the number of bond one has to break to have global breakdown becomes smaller and smaller. Moreover it is worth to note that, apart the shape of $\phi(x)$ and the behavior of $\langle x \rangle(t)$, all the other statistical properties of the system do not depend on the used weakening rule.

Finally, it is worth to point out that, to our knowledge, apart the qualitative results of [2], no quantitative experimental results are available. For example, a measurement of the fractal dimension of cracks or their size distribution would be extremely useful to further test the predictions of this model. At the moment, this model seems able to capture, with its extremely simplified dynamics, some basic properties of fracturing processes.

In conclusion, we have presented a new model for fractures, which is useful in describing in a semi-quantitative way some basic mechanism in drying paint-like and mud-like cracking processes, for extremely thin samples. Due to its extreme simplicity, the model is particularly suitable for large scale simulations and takes into account the damaging effects involved in fracture propagation. Even in this simple model we are able to analyze which conditions trigger SOC behavior in such systems. Furthermore, the change in the threshold distribution, induced by the damaging mechanism, allows us to write down explicitly the form of the breakdown probability for the bonds of the sample. Possible further research could consist, for damaging rule **2**, in a more refined calculational scheme, in which two variable probability densities are also considered. This would be the first order correction to our MF approach considering only one-variable distributions, and could allow us to take into account correlations induced by the damaging rule. Such a generalization of the RTS theory, formally discussed in [17], is however technically very difficult. Another research direction we are following is the application of real space techniques, combined with the RTS approach, to calcu-

late the critical exponents of the model. The authors acknowledge the support of the EU grant Contract No. FMRXCT980183.

APPENDIX A: RTS FOR THE DAMAGED SYSTEM

In this appendix a simple explication of the RTS probabilistic equations is provided.

First of all, one has to note that in this kind of models (as well as in Invasion Percolation) the initial condition of the system is characterized by independent variables (the breaking thresholds of the bonds) identically and uniformly distributed.

However, once the minimal value in the set is found and the relative bond broken, the knowledge of this event makes the variables of the remaining non-broken bonds no longer simply uniformly distributed in the interval $[0, 1]$, and correlated (no more independent one each other). In fact, after the breaking of the bond with the minimal threshold, one has to *condition* the probability of any further event to the last known event. This information influences the probability distribution of the remaining bonds of the system and creates correlations among them [19].

The systematic study of this “memory” effect is what is called Run Time Statistics [6,17].

In order to clarify the “step by step” mechanism of storage of conditional information, let us think to have fixed a time-order path A_t , i.e. an *history* of the dynamics up to time t . A_t is given by the time ordered sequence $\{i_0, i_2, \dots, i_{t-1}\}$ of the broken bonds up to time t . Let us suppose to know the joint threshold probability density function $P_t(\{x\}_{\partial C_t}|A_t)$ of the whole set of non-broken bonds conditioned to the knowledge of the past history A_t . $P_t(\{x\}_{\partial C_t}|A_t)$ represents the “effective” distribution of the disorder at the t^{th} time-step of a fixed history A_t . Note that at time $t = 0$, one has:

$$P_0(\{x\}_{\partial C_0}) = \prod_{k \in S} p_0(x_k) = 1, \quad (\text{A1})$$

where S is the whole lattice, as no information from the dynamics is still present.

Since any kind of “order” relation, superimposed to a set of independent stochastic variables, introduces correlations, in general $P_t(\{x\}_{\partial C_t}|A_t)$ does not factorize in the product of single-bond “effective” density functions for $t > 0$ [19]. That is, it is not possible to write:

$$P_t(\{x\}_{\partial C_t}|A_t) = \prod_{k \in \partial C_t} p_{k,t}(x_k). \quad (\text{A2})$$

However, as shown in [18], in the limit of large number of variables the “geometrical” correlations in $P_t(\{x\}_{\partial C_t}|A_t)$ become negligible, and one can make, at any time step,

the approximation given by Eq. (A2). Therefore, we consider the approximated case where the “effective” probability density function of the disorder of the system, with all the information about the past history stored, is given by the set of “effective” one-bond functions $p_{k,t}(x)$ for each non-broken bond k . The rigorous exposition of RTS, by using the non-factorizable function $P_t(\{x\}_{\partial C_t}|A_t)$ at each t is given in [17].

Knowing the set of functions $p_{k,t}(x)$, one can write the “effective” probability $\mu_{i,t}$ that a given bond i of the set is broken at that time. It is simply the probability, conditioned to the whole past history, that x_i is the minimum in the set of non-broken bond variables. Consequently, it is given by Eq. (1), i.e.

$$\mu_{i,t} = \int_0^1 dx p_{i,t}(x) \left[\prod_{k(\neq i)}^{\partial C_t} \int_x^1 dy p_{k,t}(y) \right]. \quad (\text{A3})$$

The set of $\mu_{i,t}$ for each non-broken bond and for each time-step, defines a branching process of the dynamics; i.e. each history A_t at time t continues with a certain probability $\mu_{i,t}$ in a different history A_{t+1} at time $t + 1$ for each breaking bond i at time t . In order to continue the probabilistic description of the branching at further time-steps, one should obtain the new set of functions $p_{k,t+1}(x)$ for these different cases of breaking at time t , using only the “old” set of $p_{k,t}(x)$ and the set of probabilities $\mu_{i,t}$ defining the branching. This is possible by using the notions of conditional probability. Here the simple rule relating the conditional to joint probability of a first event A to a second event B is reminded [19]:

$$\text{Prob}(A|B) = \frac{\text{Prob}(A \cap B)}{\text{Prob}(B)}, \quad (\text{A4})$$

where, as usual, $A|B$ means the event A *conditioned* to the event B , while $A \cap B$ the event A *joint* to the event B .

Note that “memory” up to time t , for a fixed history A_t in the branching of all the possible histories, is already stored in the functions $p_{k,t}(x)$. Consequently, in order to obtain the set of probability functions $p_{k,t+1}(x)$ for the history A_{t+1} obtained from A_t adding the breaking of bond i at time t , one has to store only information about the last step.

At this point one has to distinguish the three cases: **(1)** the just broken bond i , **(2)** a non-broken bond j far from i , and **(3)** a non-broken neighbor l of i .

(1) In this case let us call the conditioned probability density of bond i after its breaking with $m_{i,t+1}(x)$ instead of $p_{i,t+1}(x)$, remarking with this that after its breakdown, bond i is removed definitely from the interface. Note that, since after t the bond i does not participate to the dynamics, its “effective” probability density will not change anymore. $m_{i,t}(x)dx$ is the probability that $x < x_i \leq x + dx$, conditioned to the the past history up

to its breaking. However, since the memory up to the time-step just before its breaking is stored in the known functions $p_{k,t}(x)$, $m_{i,t}(x)dx$ is the probability, calculated using the set of functions $\{p_{k,t}(x)\}$, that $x < x_i \leq x + dx$ (event A of Eq. (A4)) conditioned to the fact that the bond x_i is the minimum in the set of interface bonds at that time (event B of Eq. (A4)). Therefore, from Eq. (A4), one has Eq. (2):

$$m_{i,t+1}(x) = \frac{1}{\mu_{i,t}} p_{i,t}(x) \left[\prod_{k(\neq i)}^{\partial C_t} \int_x^1 dy p_{k,t}(y) \right]. \quad (\text{A5})$$

In a quite similar way we can update the effective probability densities for the cases **(2)** and **(3)**. In the case **(2)**, using the set of functions $\{p_{k,t}(x)\}$, $p_{j,t+1}(x)dx$ is the probability that $x < x_j \leq x + dx$ (event A) conditioned to the fact that x_i was the minimal in the interface at time t . Again from Eq. (A4) one has Eq. (3):

$$p_{j,t+1}(x) = \frac{1}{\mu_{i,t}} p_{j,t}(x) \int_0^x dy p_{i,t}(y) \left[\prod_{k(\neq i,j)}^{\partial C_t} \int_y^1 dz p_{k,t}(z) \right]. \quad (\text{A6})$$

In the case **(3)** one has to distinguish the two different damaging rules, and the conditioning events are more complex. For rule **1**, using the set of function $\{p_{k,t}(x)\}$, $p_{l,t+1}(x)dx$ is the probability that $x < x_l \leq x + dx$ (event A) conditioned to the fact that x_i was the minimum and that the value of x_l at this time-step differs from the value at the previous time-step for a random fraction of itself (event B). One, then, gets Eq. (4):

$$p_{j,t+1}(x) = \frac{1}{\mu_{i,t}} \int_0^1 dy \frac{1}{y} \theta(y - x) p_{j,t}(y) \times \int_0^y dz p_{i,t}(z) \left[\prod_{k(\neq i,j)}^{\partial C_t} \int_z^1 du p_{k,t}(u) \right]. \quad (\text{A7})$$

Finally, for rule **2**, always using the set of functions $\{p_{k,t}(x)\}$, $p_{l,t+1}(x)dx$ is the probability that $x < x_l \leq x + dx$ (event A) conditioned to the fact that x_i was the minimum and that the value of x_l at this time-step differs from the value at the previous time-step for a fraction $1/n_{i,t}$ of x_i (event B). From this one has eq. (5):

$$p_{j,t+1}(x) = \frac{1}{\mu_{i,t}} \int_0^1 dy \left[\prod_{k(\neq i,j)}^{\partial C_t} \int_y^1 dz p_{k,t}(z) \right] p_{i,t}(y) p_{j,t}\left(x + \frac{y}{n_{i,t}}\right) \times \theta\left(\frac{n_{i,t}}{n_{i,t}-1}x - y\right) \theta(n_{i,t}(1-x) - y). \quad (\text{A8})$$

- [1] A. Gabrielli, R. Cafiero, G. Caldarelli *Europhys. Lett.* **45**, 13 (1999) (1990).
- [2] A. Groisman and E. Kaplan, *Europhys. Lett.* **25** 415, (1994).
- [3] D. Wilkinson, J. F. Willemsen *J. Phys. A (London)* **16** 3365, (1983).
- [4] G. Caldarelli, C. Castellano, A. Vespignani *Phys. Rev. E* **49** 2673, (1994); G. Caldarelli, F. D. Di Tolla, A. Petri *Phys. Rev. Lett.* **77** 2503, (1996).
- [5] S. Zapperi, A. Vespignani, H. E. Stanley *Nature* **388** 658, (1997).
- [6] M. Marsili *J. Stat. Phys.* **77** 773, (1994); A. Gabrielli, R. Cafiero, M. Marsili and L. Pietronero *Europhys. Lett.* **38** 491, (1997).
- [7] H. J. Herrmann, S. Roux (eds) *Statistical Models for the Fractures of Disordered Media*, North Holland (1990).
- [8] D. Sornette, C. Vanneste *Phys. Rev. Lett.* **68** 612, (1991).
- [9] Bazant Z. P., Carol I. (eds), *Creep and Shrinkage of Concrete E & FN Spon* (1993).
- [10] J. T. Neal, *Geol. Soc. Am. Bull.* **76** 1075, (1966); J. T. Neal and W. S. Motts, *J. Geol.* **75** 511, (1967); G. Korvin, *Pure. Appl. Geophys.* **131** 289, (1989).
- [11] J. Walker, *Sci. Am.* **255** 178, (1986).
- [12] F.H. Wittmann, A. Slowik, A. M. Alvaredo, *Materials and Structures* **27** 499, (1994); T. Nishikawa, M. Takatsu *Cement and Concrete Research* **25** 1218, (1995).
- [13] J. Hoshen and R. Kopelman, *Phys. Rev. B* **14**, 2428 (1976).
- [14] A. Petri, G. Paparo, A. Vespignani, A. Alippi, M. Costantini *Phys. Rev. Lett.* **73** 3423, (1994).
- [15] P. Bak, C. Tang, K. Wiesenfeld *Phys. Rev. Lett.* **59** 381, (1987).
- [16] P. Bak, K. Sneppen *Phys. Rev. Lett.* **71** 4083, (1993).
- [17] A. Gabrielli, "Memory effects in stochastic growth dynamics with quenched disorder: the Generalized Run Time Statistics", in preparation.
- [18] R. Cafiero, A. Gabrielli and M. Marsili, *Phys. Rev. E* **55**, 7745 (1997).
- [19] W. Feller, *An Introduction to Probability Theory and its Applications*, vols. 1 and 2, ed. J. Wiley & Sons, (New York, 1965).

	$L = 64$	$L = 128$	$L = 256$
D_f (dam. rule 1)	1.75(2)	1.74(2)	1.74(2)
D_f (dam. rule 2)	1.73(2)	1.75(2)	1.76(2)

TABLE I. Fractal dimension of the spanning cluster for different sizes and for the two damaging rules.

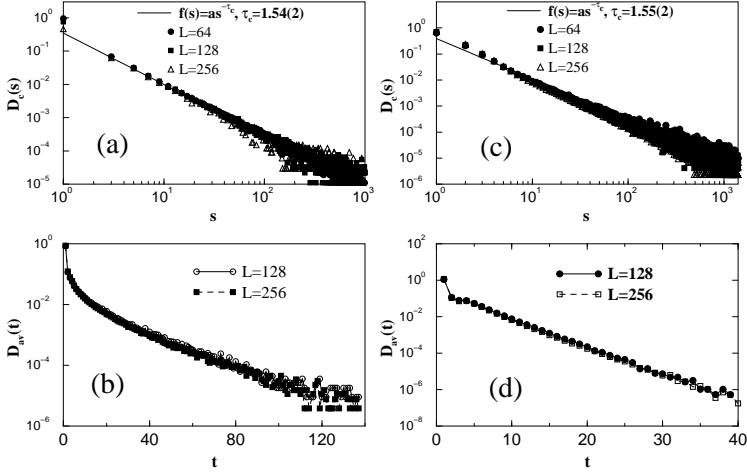


FIG. 1. (a): Probability distribution ($\log_{10}\text{-}\log_{10}$ plot) $D_c(s)$ of the cluster size, for $L = 64, 128, 256$. (b): Avalanche size distribution (linear- \log_{10} plot) $D_{av}(t)$ for $L = 128, 256$. (c) and (d): The same quantities for the weakening rule **2**.

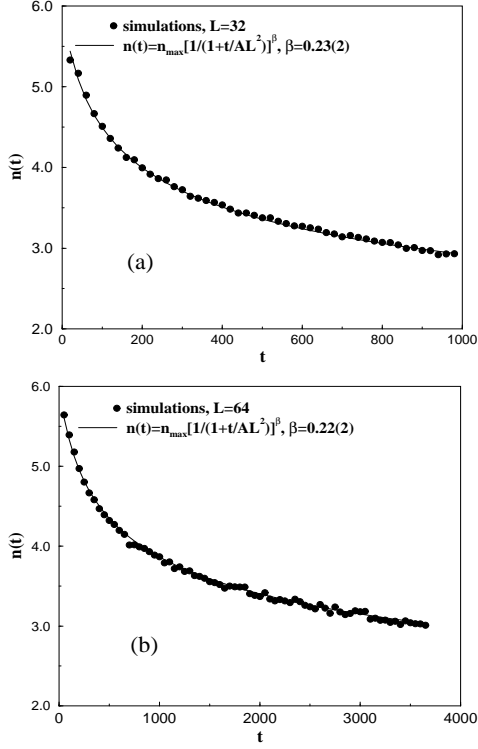


FIG. 2. fit of $n_t(L)$ with the scaling form 15 (weakening rule **1**) for $L = 32$ (a) and $L = 64$ (b).

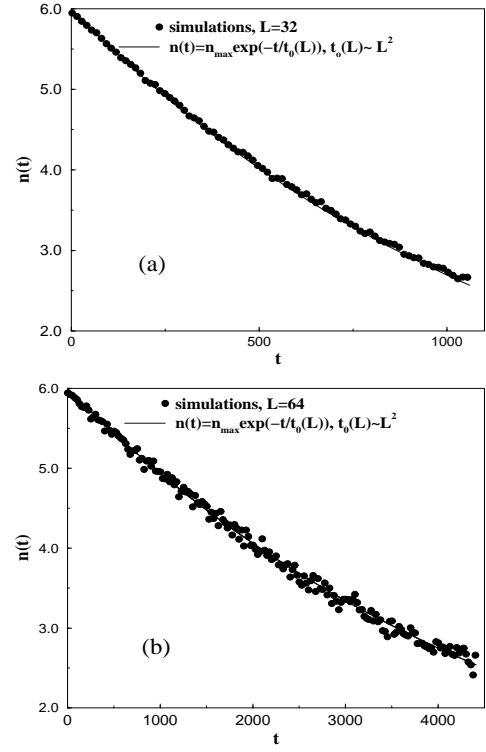


FIG. 3. fit of $n_t(L)$ with the scaling form 15 (weakening rule **2**) for $L = 32$ (a) and $L = 64$ (b).

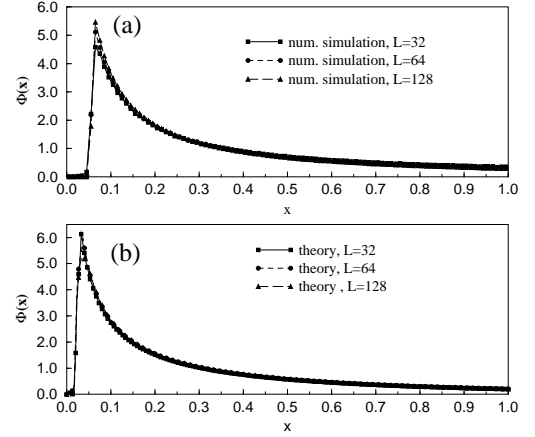


FIG. 4. Solution of Eq. 13 for the histogram $\phi_t(x)$ at the spanning time (b), compared with simulations (a), for the weakening rule **1**.

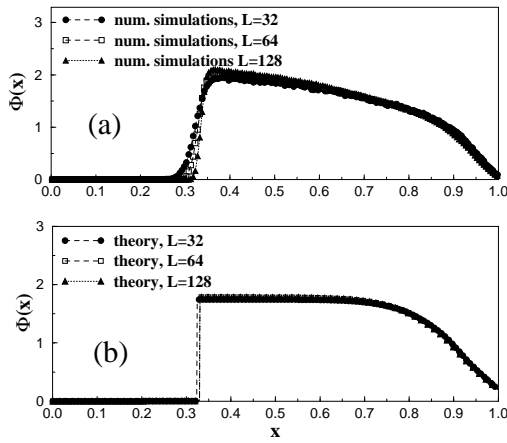


FIG. 5. Solution of Eq. 13 for the histogram $\phi_t(x)$ at the spanning time (b), compared with simulations (a), for the weakening rule 2.

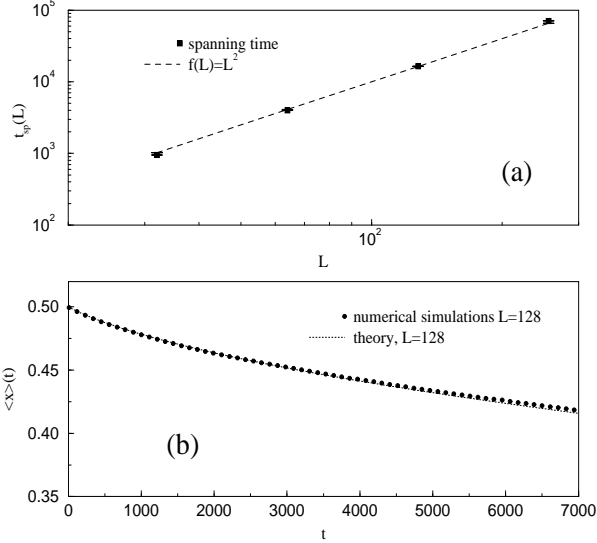


FIG. 6. (a) Spanning time versus system size L for weakening rule 1. One can see a nice agreement with the expected scaling law $t_{sp}(L) \propto L^2$. (b) Solution of Eq. 18 compared with numerical simulations.

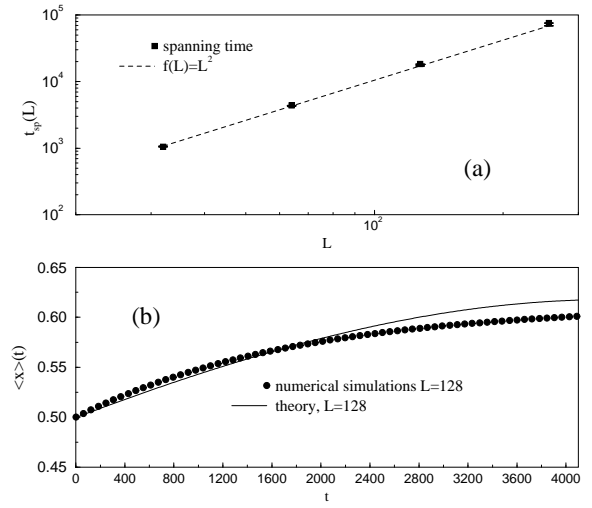


FIG. 7. (a) Spanning time versus system size L for weakening 2. Also in this case, there is very good agreement with the expected scaling law $t_{sp}(L) \propto L^2$. (b) Solution of Eq. 19 compared with numerical simulations.